SiF 2018– The 10th International Conference on Structures in Fire
FireSERT, Ulster University, Belfast, UK, June 6-8, 2018

CFD ANALYSES USED TO EVALUATE THE INFLUENCE OF COMPARTMENT GEOMETRY ON THE POSSIBILITY OF DEVELOPMENT OF A TRAVELLING FIRE

Marion Charlier[1], Antonio Gamba[2], Xu Dai[3], Stephen Welch[3], Olivier Vassart[1], Jean-Marc Franssen[2]

ABSTRACT

The response of structures exposed to fire is highly dependent on the type of fire that occurs, which is in turn very dependent on the compartment geometry. In the frame of the European RFCS TRAFIR project, CFD simulations using FDS software were carried out to analyse the influence of compartment geometry and the interaction with representative fuel loads to explore the conditions leading to the development of a travelling fire. The influence observed of ceiling height, crib spacing, and opening geometry in controlling spread rates tend to confirm the possibility to predict the occurrence or not of travelling fire. In a subsequent step, the radiative intensities and gas temperatures calculated by FDS have been used by SAFIR® to calculate the temperatures in steel structural elements located in the compartment and the structural behavior of a frame made of these elements.
Keywords: CFD, Fire scenario, Travelling fire, Coupling FDS-SAFIR®

1 INTRODUCTION

Small compartment fires behave in a relatively well understood manner, usually defined as post-flashover fires, where the temperatures within the compartment are considered to be uniform. Yet, fires in large compartments do not always reach a post-flashover fire state and there is instead a more localised fire that may travel within the compartment. More recently, the “travelling fire” terminology has been used to define fires burning locally and moving across entire floor plates over a period of time [1]. Several studies have been presented about the behaviour of a structure when it is subjected to a travelling fire ([2], [3], [4]). These experimental campaigns provide first insights regarding the parameters influencing fire spread, such as heat release rate density and wood moisture content. Furthermore, in 2005, Thomas [5] set an experimental program in a deep enclosure and the main conclusion was that fires in deep compartments are strongly affected by the ventilation. Nevertheless, no proper information or scientific knowledge has been established yet on the configurations that can lead to the development of travelling fires [6]. In the frame of TRAFIR project, several CFD numerical simulations were made to identify and attempt to quantify the parameters that may lead to a travelling fire. This paper presents some of these simulations and explains how the CFD results can be used to perform a numerical analysis of the temperature development and resulting mechanical behaviour of a steel structure that considers comprehensively the travelling nature of the fire.

[1] ArcelorMittal Global R&D, Luxembourg.
e-mails: marion.charlier@arcelormittal.com and olivier.vassart@arcelormittal.com
[2] Department of Architecture, Geology, Environment & Constructions (ArGEnCo), Liege University, Belgium.
e-mails: antonio.gamba@uliege.be and jm.franssen@ulg.ac.be
[3] School of Engineering, BRE Centre for Fire Safety, The University of Edinburgh, United Kingdom.
e-mails: x.dai@ed.ac.uk and s.welch@ed.ac.uk

2 THE SETUP OF FDS SIMULATIONS AND ITS CORRESPONDING ASSUMPTIONS

The Fire Dynamics Simulator (FDS) [7] is adopted as numerical simulation tool. The conditions examined in this work are confined to the initial localised and spreading phase of the fire. In the simplified hypothesis of a well-stirred reactor leading to a uniform situation in the compartment, under-ventilated conditions do not prevail. In the hereafter described analyses, the use of CFD allows to consider in detail the different aspects of fluid mechanics and highlight that the fire may be under-ventilated at certain moments in some regions of the compartment.

2.1 Grid size

The cell size used in the FDS models depends highly on the situation that is modelled and on the purpose of the simulation. For simulations involving buoyant plumes, FDS User's Guide [7] defines a non-dimensional parameter to assess the quality of the mesh: $D^*/\delta x$. In all the hereafter described simulations, cell size of 0.25m x 0.25m x 0.25m was considered. These values were not based on a sensitivity analysis but on existing analyses representing fire dynamics in large enclosures. Indeed, the FDS Validation Guide contains a table of the values of $D^*/\delta x$ used in the simulation of the validation experiments and were used as guidance. Furthermore, for all the FDS models presented hereafter, the cell size is smaller than the suggested fine cell size recommended by the "Mesh Size Calculator" [8] tool developed by Kristopher Overholt. Extra cells have been defined outside the compartment boundaries in order to consider the coupling to the external environment.

2.2 Representation of fuel

The fire load is supposed to be made of discrete wood cribs. No detailed representation of a wood crib (i.e. involving alternation of sticks and air gap) was used but a simpler approach was adopted, using 1m^3 solid cubes. This approach is based on the work done by Degler & Eliasson [9]. The overall heat release rate was used as input to VENTs with each VENT representing a wood crib burning surface. The wood constituting the cubes is red oak type with the following chemical composition: $C_{3.4}H_{5.78}O_{2.448}N_{0.0034}$ and a soot yield of 0.0015 [g/g]. These values are adopted from the SFPE Handbook [10]. The properties of the modelled wood are: conductivity 0.1 W/m/K, specific heat 1.3 kJ/kg/K, emissivity 0.9 and density 400 kg/m^3. The predefined HRR curve considered come from Degler & Eliasson's work [9]: it was first obtained numerically using complex pyrolysis model in FDS then validated by comparison with pallet HRR curves obtained experimentally. The HRR curve has a peak at 480 [kW/m^2] and lasts for 33 minutes.

2.3 Fire spread

Planar devices were placed on each faces of the cribs (except on the face in contact with the floor) to measure the temperatures on the solid surfaces. If the surface temperature reaches 300°C on at least one face of the volume, then the five surfaces start burning following the prescribed HRR curve. This temperature of ignition was arbitrarily set equal to 300°C, which is a reasonable approximation of ignition temperature for certain cellulosic materials [10].

2.4 Openings and boundary walls

The openings represented in the models are present from the beginning of the fire. Walls and ceiling are made of 25 cm thick concrete (conductivity 2.4 W/m/K, specific heat 1 kJ/kg/K, density 2400 kg/m^3). In all the compartments presented in this paper, openings are present on both walls along the X axis, and centred. For the sake of clarity, X and Y axis mentioned hereafter correspond respectively to the horizonal and the vertical axis of plan views of the compartments.

3 RESULTS OF FDS SIMULATIONS

Different typologies of large compartments were modelled: the conditions supporting travelling fire development are explored by varying some of the fundamental inputs to the model, i.e. ceiling height, opening size, fuel load density and compartment layout. Two series of configurations are

investigated, in which series 1 relates to a deep rectangular compartment and series 2 relates to a large square compartment.

Table 1. Different configurations of large compartments

Configuration	Compartment dimensions x,y,z	Opening size	Opening factor [11]	Separation between the solid cubes (cribs)
1.a	50m x 10m x 4m	45m x 3.5m	0,20 $m^{1/2}$	1m
1.b	50m x 10m x 4m	20m x 3.25m	0,08 $m^{1/2}$	1m
2.a	20m x 20m x 8m	16m x 6.75m	0,26 $m^{1/2}$	2m
2.b	20m x 20m x 3.5m	16m x 2.25m	0,05 $m^{1/2}$	2m

3.1 Deep rectangular compartment – 1D spread

In configuration 1, a 50m x 10m x 4m compartment is defined in a model domain of 60m x 12m x 5m. The openings extend vertically from 0.25m above floor level. In both configurations (1.a and 1.b) the fire starts by the ignition of the wood crib placed at the left-end of the compartment, at mid-width (see *Fig. 1*). According to *Fig. 2*, in configuration 1.a the fire spreads slowly at the beginning (0m – 15m), then faster (15m – 50m) when the effects of pre-heating by radiation from the hot layer become more significant. Specifically, at beginning of the fire (0 – 20 minutes), the pattern of the burning area indicates a t^2 development, but the acceleration is soon damped with the remaining spread being closer to a steady rate of increase along the length of the compartment. Steady spread can be expected when the process is being driven primarily by local crib-to-crib spread and where the effects of preheating from the hot layer to cribs ahead of the front is relatively minor, and does not significantly increase with time. Also, the fire spread front edge has a clear time lag when it is in the area near the openings, as depicted on *Fig. 2* around y=0m and y=10m. This may be due to the fact that in those areas the pyrolysis is moderated by exposure to the adjacent cold ambient air and the main combustion zone at the diffusion interface in the gas phase is not moving ahead of the pyrolysis zone. As shown in *Fig. 2* and *Fig. 3*, the fire spreads much faster overall under configuration 1.b compared with configuration 1.a. Indeed, configuration 1.b requires 52 minutes to spread over the whole compartment compared to 90 minutes for configuration 1.a. This can be explained by more energy leaving the compartment through the larger openings of configuration 1.a. Compared with configuration 1.a, the compartment of configuration 1.b is more likely to increase the fire spread rate, due to greater retained heat but also due to the burning zone seeking oxygen towards the openings (0m – 10m).

Some interesting differences are also apparent in the instantaneous fire spread rate evolution. The speed at the horizontal centreline, versus X location, is directly represented in *Fig. 4*. The values are determined from the straight-line distance between two ignited wood crib centres (mm) divided by the time for the second wood crib being ignited (s) and for each of these values, the depicted relative X location corresponds to the mid-distance between two ignited wood cribs. Thus, higher velocity regions of the chart represent rapid transitions between cribs, but are of relatively short duration. In configuration 1.b when the fire has passed the opening (10m – 20m), more oxygen is available to sustain more vigorous combustion, and compensating to some extent for the reduction in retained heat. This may be part of the reason that the fire spread rate is higher in this region, compared with the region from 0m – 10m. Then the fire spread rate decreases from 30m – 35m as access to oxygen diminishes towards end of opening. In configuration 1.b, at the region of 35m – 50m, the fire spread rate increases again, due to heat retention in the more enclosed region, though much of the gas-phase combustion may still be located near the opening at around 35m. Moreover, as shown in *Fig. 4*, the fire spread rate in configuration 1.b is at times significantly higher than the one in configuration 1.a. Overall, compared to the more open configuration 1.a, the fire travel

format in configuration 1.b is less steady, being strongly influenced by phenomena associated with the smaller openings.

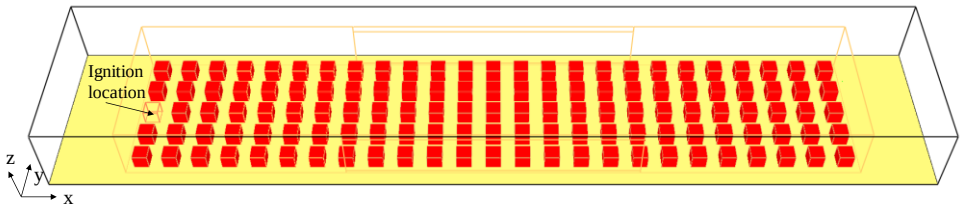

Fig. 1: Model of configuration 1.b

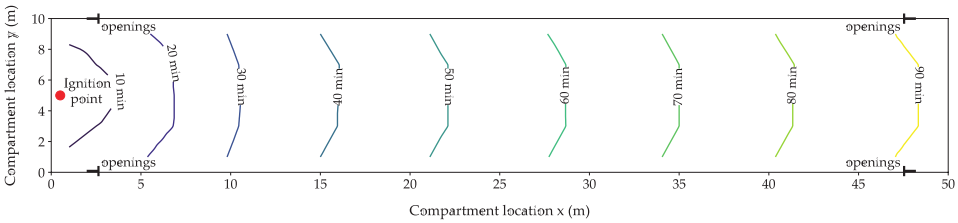

Fig. 2: Fire spread time vs. compartment location, under configuration 1.a

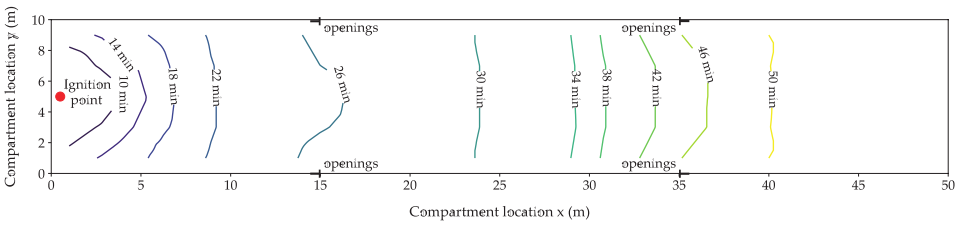

Fig. 3: Fire spread time vs. compartment location, under configuration 1.b

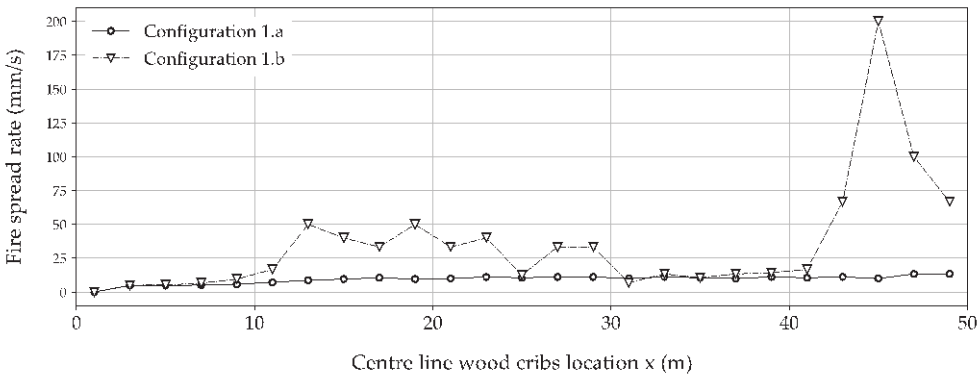

Fig. 4: Fire spread rate vs. compartment location, under configurations 1.a and 1.b

3.2 Square compartment – 2D spread

In configurations 2.a and 2.b, the compartment dimensions are respectively 20m x 20m x 8m and 20m x 20m x 3.5m and the model domains respectively 21m x 21m x 9m and 24m x 24m x 4m. The openings are placed 0.25m above floor level. The fire starts by the ignition of the wood crib placed at the centre of the compartment and the fire load consists of 1m^3 wood cribs spaced 2m away from each other. This fuel density was chosen to represent the rate of heat release density of an office building prescribed by EN1991-1-2 Annex E [11], which is 250 kW/m^2. When compared with configurations 1, the results indicate generally slower spread rates, which is consistent with the greater crib spacing. Also, a 2D spread is observed in both cases, but with a slightly slower spread

at the openings side for configuration 2.a where less heat is retained, as depicted in *Fig. 5.a*. In configuration 2.b the fire spread accelerates more rapidly, taking 28 minutes to spread over the entire floor versus 45 minutes in configuration 2.a. This difference is suggested to result mainly from lowering the ceiling height, due to the stronger coupling between the hot gases and the pyrolyzing cubes. The change of opening factor also impacts on the ventilation airflows at the openings, and the more regular spread depicted on *Fig. 5.b* is a net result of the enhanced heat transfer with the lower ceiling together with changes in burning behaviour related to ventilation differences and the reduced overall duration of spread.

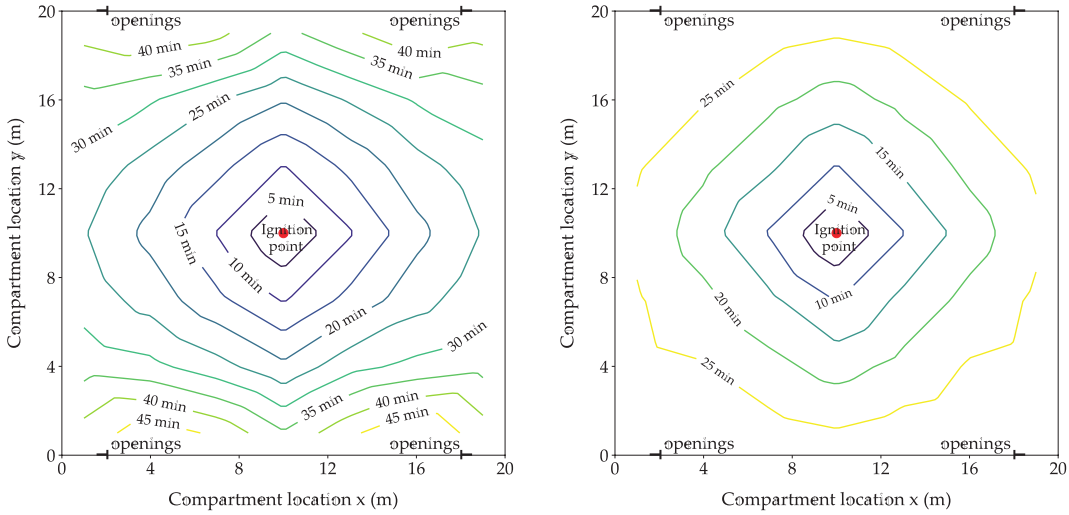

Fig. 5: Fire spread time vs. compartment location under a) configuration 2.a; b) configuration 2.b

4 LINKING CFD AND FEM WHILE COUPLING FDS AND SAFIR SOFTWARES

The CFD analyses are performed with a model of the compartment that does not necessarily contain the structural elements [12]. Structural elements must be present in the CFD model if they form a boundary of the fire compartment (walls and ceiling slab) or if they significantly influence the mass flow or the radiative flow in the compartment (deep concrete beams, wide columns, shear walls…). If the structure is made of linear steel members, it is likely that the characteristic size in the transverse direction of the steel elements is small with respect to the characteristic length of the compartment, which can justify the absence of these elements in the CFD domain. A dedicated version of FDS 6 has been written where the sole modification is the creation by FDS of a new file in which particular results are written to be used by the subsequent structural analysis by SAFIR [13]. The results are:

- *gas temperature*, used for the convective heat transfer to the structural elements;
- *coefficient of convection*, depends on the gas velocity. NB – SAFIR does not currently use this coefficient; it uses a constant value, for example 35 W/m²K, for simplicity;
- *Radiation intensity in several directions*. These intensities have been preferred to the impinging flux or the adiabatic surface temperature for different orientations, because these latter quantities both result from an integral on a surface and the information about the direction of the impinging intensities considered in these integrals is lost, with the consequence that concave sections cannot be considered appropriately.

In order to reduce the size of this transfer file, the time steps, the spatial steps in the 3 directions, as well as the limits of the domain covered in the file, do not necessarily coincide with the respective values of the CFD analysis. Linear interpolations are used by FDS between its internal results to write the file, and linear interpolations are performed by SAFIR when reading the file to compute the relevant values at the requested positions in time and in space. Based on the data found in the transfer file, a series of 2D transient thermal analyses are performed along the structural members

and the results are stored in appropriate files. As these 2D temperature distributions will be used subsequently to represent the temperature in beam finite elements, a temperature distribution is calculated for each longitudinal point of integration of each beam finite element; SAFIR uses 2 or 3 points of Gauss along the beam elements. In these 2D thermal analyses, the impinging flux is computed for each boundary (in the sense of finite element discretisation) of the section, depending on its orientation. As an approximation, the position of the boundaries of the section in the fire compartment is the same for all boundaries of a section (at the position of the node line of the beam finite element, based on the assumption that half of the characteristic length of the section is small with respect to the size of the compartment). For the boundaries on concave parts of the section, impinging radiative intensities from certain direction are discarded if there is an obstruction by other parts of the section. Mutual radiation between different boundaries of the section in the concave regions is not considered.

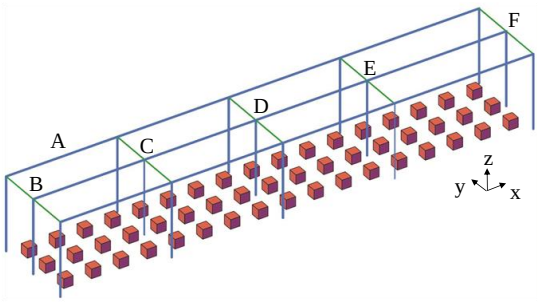

Fig. 6: Steel structure in the compartment and solid cribs

In order to illustrate the capabilities of the CFD-FEM coupling, the steel structure shown on *Fig. 6* is supposed to be present in a compartment similar to the one depicted in *Fig. 1*, i.e. a 51m x 9m x 4m compartment with 20m x 3.25m opening size. The solid cribs are spaced 2m away from each other to represent the rate of heat release density of an office building, which is 250 kW/m^2 [11]. *Fig. 7.a* shows the isotherms after 41 minutes in the IPE400 beam in the middle of the first span (point A in *Fig. 6*). A clear difference is observed between the lower flange and the upper flange, the latter being exposed to fire only on 3 sides. A gradient can also be observed in the flanges from right (toward the centre of the compartment) to left (toward the wall). Also, the lower part of the web is somehow protected by the lower flange from the radiation intensities that come mainly from the bottom right direction (i.e. the ground in the compartment). *Fig. 7.b* shows the evolution of the temperature in the centre of the section in the central beam (from B to F) after 67 and 92 minutes. The offset between the plots reflects the spread of the fire in the compartment.

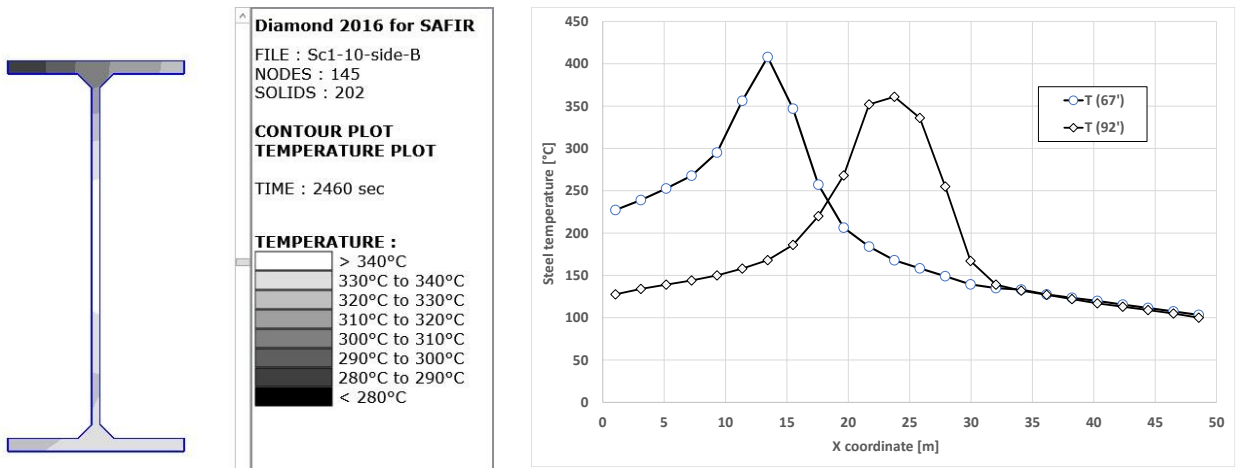

Fig. 7: Steel temperatures in beams. a) Isotherms after 41 minutes at A; b) Evolution along central beam B-F

The temperatures computed in the sections of the 3D beam finite elements that form the structure are taken into account in a geometrically transient and materially nonlinear structural analysis performed with SAFIR. Many different results can be obtained from this type of analysis, such as the evolution of axial forces and bending moments in the elements, the stresses in the elements, the displacements of the nodes and finally, the fire resistance time and the failure mode (or the absence of failure). The evolution of the vertical displacement at the top of the five columns from the central frame is represented on *Fig. 8*. As the structure does not collapse, the vertical displacement is essentially elastic and is therefore a result of thermal elongation. The travelling nature of the fire is highlighted by the time shift of the thermal elongation in the columns B to F.

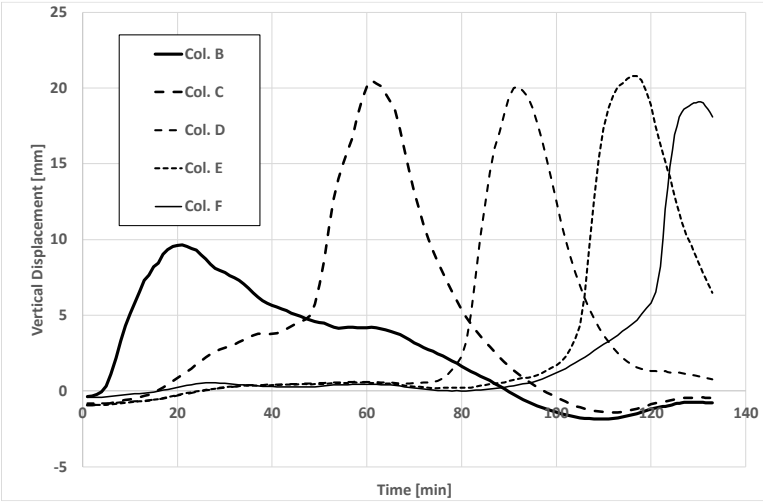

Fig. 8: Evolution of the elongation of the columns in the central frame as a function of time

5 DISCUSSIONS AND FURTHER IMPROVEMENTS

The sample cases presented illustrate the potential value of CFD for generating and analysing fire dynamic conditions which influence the likelihood of fire spread. It is important to note that these are numerical examples and not validation studies. Thus there are important provisos on the interpretation of the results. Further work would be required to quantify any deviations arising due to numerical effects. Also, concerning the methodology used for the representation of burning fuel, Degler & Eliasson [14] highlight that it presents some drawbacks. Before a cell reaches the ignition temperature, its heating is computed while considering heat exchanges with the environment. But as soon as the ignition temperature is met, FDS represents the fire by releasing volatile combustibles which, if all are burnt, results in the prescribed HRR curve. This is done without considering the evolution of heat exchange with the environment. Moreover, the uniform cubic shape of the obstruction prevents air flow through the object. Nevertheless, it was concluded that this approach can yield a good representation of a burning wood crib in comparison with hand calculations of the upper and mean value of the mass loss rate [13]. In next steps, different ignition locations will be considered and FDS results will be analysed to highlight the spread of cribs extinction. Furthermore, the details of glazing failure have been ignored at this stage, and more realistic compartment geometries and boundary materials should also be considered. Moreover, having demonstrated the value of the methodology, further systematic use of numerical simulations will be undertaken to perform more comprehensive parametrical analyses. The calibration of these simulations will also benefit from experimental tests from the literature or to be performed in the frame of the TRAFIR project. It will then be possible to determine the conditions in which a travelling fire may develop, or not, and therefore inform on appropriate fire scenarios to be considered. In the analysis performed to calculate the temperature in the structure, it would be possible to consider the real position of each boundary of the sections instead of approximating this

position to the centre of the section. Parallelisation of the code, which is currently under way, will reduce the CPU time requested for the large number of 2D thermal analyses performed in the sections.

6 CONCLUSIONS

Using Fire Dynamics Simulator, different geometrical arrangements were modelled in terms of compartment layout, opening size and ceiling height. A fire load composed of wood cribs has been considered using discrete volumes arranged on regular grids and a temperature criterion on the volume surfaces was used to trigger the start of a predefined heat release curve. It has proved possible to extract from CFD results quantitative measures of fire behaviour, in particular the fire spread rates. It was possible to interpret all the observed trends in terms of fundamental principles of fire dynamics. Such method is built on several explicit assumptions but permits a first assessment of the conditions required for fire spread and provides an indication of some of the influential parameters and likely sensitivities. Further, by considering the detailed results of the CFD analysis in a nonlinear thermomechanical analysis of a structure located in the fire compartment, the coupling of the structural response to the travelling fire characteristics has been demonstrated.

ACKNOWLEDGMENT

This work was carried out in the frame of the TRAFIR project with funding from the Research Fund for Coal and Steel (grant N°754198). Partners are ArcelorMittal Belval & Differdange, Liège Univ., the Univ. of Edinburgh, RISE Research Inst. of Sweden and the Univ. of Ulster.

REFERENCES

1. J. Stern-Gottfried, G. Rein (2012). *Travelling fires for structural design – Part I: Literature review*. Fire Safety Journal 54. pp 74-85.
2. K. Horová, T. Jána, F. Wald (2013). *Temperature heterogeneity during travelling fire on experimental building*. Advances in Engineering Software 62-63. pp 119-130.
3. J.P. Hidalgo, A. Cowlard, C. Abecassis-Empis, C. Maluk, A.H. Majdalani, S. Kahrmann, R. Hilditch, M. Krajcovic, J.L. Torero (2017). *An experimental study of full-scale open floor plan enclosure fires*. Fire Safety Journal 89. pp 22-40.
4. D. Rush, D. Lange, J. Maclean, E. Rackauskaite (2015). *Effects of a Travelling Fire on a Concrete Column – Tisova Fire Test*. Proceedings of the 2015 ASFE Conference.
5. I. Thomas, K. Moinuddin, I. Bennetts (2005). *Fire development in deep enclosure*. Proceedings of the Eighth IAFSS Symposium. pp 1277-1288.
6. X. Dai, S. Welch, A. Usmani (2017). *A critical review of 'travelling fire' scenarios for performance-based structural engineering*. Fire Safety Journal 91. pp 568–578.
7. K. McGrattan, S. Hostikka, R. McDermott, J. Floyd, C. Weinschenk, K. Overholt (2017). *Fire Dynamics Simulator User's Guide*. Sixth Edit. National Institute of Standards and Technology (NIST).
8. K. Overholt (2018). FDS Mesh Size Calculator [Online]. http://www.koverholt.com/fds-mesh-size-calc/.
9. J. Degler, A. Eliasson, A. Anderson, D. Lange, D. Rush (2015). *A-priori modelling of the Tisova fire test as input to the experimental work*. Proc. 1rst Int. Conf. on Struct. Safety under Fire & Blast, Glasgow, UK.
10. SFPE Handbook of Fire Protection Engineering (2002). Third Edition. NFPA.
11. EN1991-1-2 (2002). Eurocode 1: Actions on structures – Part 1-2: General actions-Actions on structures exposed to fire. CEN, Brussels.
12. N. Tondini, A. Morbioli, O. Vassart, S. Lechêne, J.-M. Franssen (2016). *An integrated modelling strategy between a CFD and an FE software: Methodology and application to compartment fires.* Journal of Structural Fire Engineering 7 Issue 3, pp 217-233.
13. J.M. Franssen, T. Gernay (2017). *Modeling structures in fire with SAFIR®: theoretical background and capabilities*. Journal of Structural Fire Engineering 8. pp 300-323.
14. J. Degler, A. Eliasson (2015), *A Priori Modeling of the Tisova Fire Test in FDS*, Bachelor's Thesis, Luleå University of Technology.